

VII. MICROWAVE ELECTRONICS

Prof. L. D. Smullin
Prof. H. A. Haus
Prof. S. Saito (visiting fellow)
A. Bers

R. M. Bevensee
T. J. Connor
B. W. Faughnan

C. Fried
B. A. Highstrete
A. J. Lichtenberg
C. Morgenroth

RESEARCH OBJECTIVES

The present program of this group follows two main lines. The first is a continuation of the research on noise in electron beams and a more general study of the noise in active devices. The second is a study of the problems involved in high-power beam tube design.

1. Noise. Several experiments for measuring the value of Π/S in the beams originating from "low-noise guns" are in progress. Three methods for making such a determination have been proposed, and it is hoped to try all of them by the end of the year.

The theoretical work leading to the formulation of the minimum "noise measure" for microwave beam tubes is being extended to cover all types of active devices (transistors, for example).

2. High-Power Beam Tubes. A study of the phenomena in dense, high-power beams, both solid and hollow, has been started. Both theoretical and experimental work will be carried out to determine the limits to the maximum practical beam perveances in klystrons and traveling-wave tubes.

In order to understand better the family of beam tubes, a "distributed" klystron consisting of eight closely spaced, uncoupled cavities is being built. A theoretical analysis of this kind of device is also under way.

During the coming year it is planned to make detailed studies of the efficiency of a number of commercially available, pulsed klystron amplifiers.

L. D. Smullin, H. A. Haus

A. NOISE MEASUREMENTS

1. Minimum Noise Figure of Traveling-Wave Amplifiers

We have decided to investigate the conditions under which the minimum noise figure of a traveling-wave amplifier can be realized. Previous theoretical investigations (1) indicate that the minimum noise figure is given as

$$F_{\min} = 1 + \frac{4\pi}{kT} \left[4QC f_{\max} f_{\min} \right]^{1/2} (S - \Pi)$$

In this expression, the quantity $(S - \Pi)$ is most significant, since it is an inherent characteristic of the electron gun, and is invariant to lossless beam transformations.

The measurement of these parameters required the construction of quite a bit of new equipment. This construction was completed; it includes: a movable-cavity demountable vacuum system, which does not require sliding seals; an electromagnet thirty inches in length; a radiometer modulator; and a direct-reading noise-figure indicator (2).

T. J. Connor

References

1. H. A. Haus, Noise in one-dimensional electron beams, J. Appl. Phys. 26, 560 (May 1955).
2. C. E. Chase, A direct-reading noise-figure indicator, Electronics 28, 161 (Nov. 1955).

2. Measurement of Noise Figure

In order to measure the noise parameters S and Π (introduced by H. A. Haus, of this Laboratory) of a low-perveance electron beam, parts for the tube shown schematically in Fig. VII-1 have been built and are about to be assembled.

It is anticipated that S will be determined from the maximum and minimum readings of noise power from the cavity nearest the gun, as it is moved along the beam, and that Π/S will be determined from the noise standing-wave-ratios measured by both cavities. Appropriate formulas have been derived.

Calculated cavity parameters are as follows:

f_o , resonant frequency, 3.0 kMc

Q_o (cavity), 2000 (approximate)

Q_w (window), 2000 (approximate)

M , gap coupling coefficient, 0.72

R_{SH}/Q_o , 145

Incomplete measurements on the cavities indicate that Q_o is actually about 1200, so that the loaded Q will probably be set to 830 or so by varying Q_w . This value leads to an expected maximum available gain for the two-cavity system of 3-4 db, which should yield convenient beam noise standing-wave-ratios for measurement.

R. M. Bevensee

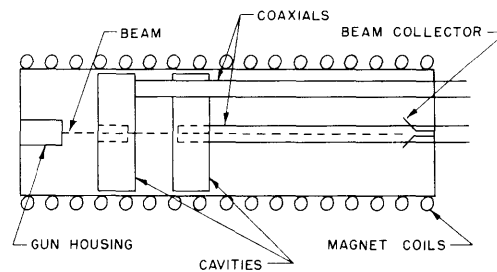


Fig. VII-1. Low-perveance beam noise-measurement tube.

(VII. MICROWAVE ELECTRONICS)

3. Beam Noise Measurement

An analysis of a new measuring method of Π/S has been carried out (1, 2). This method consists essentially of measuring the ratio of the slow wave component to the fast wave component of the electron beam noise by using a "directional beam coupler" that has the same characteristics as the conventional microwave directional coupler. With the measurement of the standing-wave-ratio of the beam noise, the ratio of Π/S can be obtained directly, independent of the value of S. Details of the analysis will be published later.

S. Saito

References

1. H. A. Haus and F. N. H. Robinson, The minimum noise figure of microwave beam amplifiers, Proc. IRE 43, 981 (1955).
2. A. Bers, Experimental and theoretical aspects of noise in microwave tubes, S. M. Thesis, Department of Electrical Engineering, M.I.T., 1955.

4. Low-Noise Traveling-Wave Tubes at 500 Mc/sec

Design of low-noise traveling-wave tubes at 500 Mc/sec has been carried out. Because of limiting the helix to a reasonable length (about one foot), the value of C had to be made as large as possible. Two structures were investigated: one with a hollow-beam gun; the other with a solid-beam gun, under the following design conditions.

1. Hollow beam

$$\begin{array}{lll} V_o = 500 \text{ volts} & \gamma_a = 2.0 & N = 11.5 \\ I_o = 14 \text{ ma} & C = 0.14 & Q = 0.4 \\ \text{Beam Dimensions} & \left\{ \begin{array}{l} 0.60 \text{ inch OD} \\ 0.55 \text{ inch ID} \end{array} \right. & \text{Gain} > 20 \text{ db} \end{array}$$

2. Solid beam

$$\begin{array}{lll} V_o = 500 \text{ volts} & \gamma_a = 0.3 & N = 11.5 \\ I_o = 300 \mu\text{a} & C = 0.07 & Q = 0.3 \\ \text{Beam Diameter} \sim 0.03 \text{ inch} & & \text{Gain} > 20 \text{ db} \end{array}$$

Construction of the hollow-beam gain is expected to start in the next quarter.

S. Saito, L. D. Smullin

B. NOISE THEORY

1. Invariants of Linear Noisy Networks

The most general linear n terminal-pair network with internal noise generators is characterized by an impedance matrix Z and an open-circuit noise-voltage column

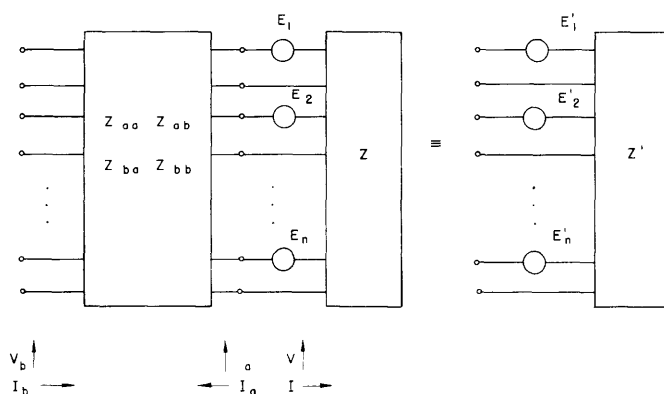


Fig. VII-2. Network transformation.

matrix E , both of n^{th} order. Introducing the terminal-voltage column matrix V and the terminal-current column matrix I , we have for the equation of the network

$$V = ZI + E \quad (1)$$

Since the Fourier amplitude of a noise process is meaningless in itself, the noise-column matrix E cannot be used directly. When meaningful information about the noise is desired, the self-power and cross-power spectra of the different noise voltages have to be used. The matrix

$$\overline{EE^+} \quad (2)$$

is a convenient summary of the spectra. The superscript $+$ indicates the operation of the Hermitian conjugate (complex-conjugate transpose) of a matrix; E^+ is a row matrix with the complex-conjugate elements of E as its elements; the bar indicates an ensemble average.

The most general transformation of an n terminal-pair network into another n terminal-pair network is shown in Fig. VII-2. The new n terminal-pair network obtained under the transformation can be characterized by a new impedance matrix Z' , and a new open-circuit noise-voltage column matrix E' . If, in particular, the $2n$ terminal-pair network used in the transformation is lossless, and therefore free of noise sources, the eigenvalues of the following matrix are left invariant in the process

$$N = \overline{EE^+} (Z + Z^+)^{-1} \quad (3)$$

The proof proceeds as follows. If the voltages and currents on one side of the transformation network are denoted by the subscript a , those on the other side by b (see Fig. VII-2) the transforming network can be characterized by the matrix relations

(VII. MICROWAVE ELECTRONICS)

$$\left. \begin{aligned} V_a &= Z_{aa} I_a + Z_{ab} I_b \\ V_b &= Z_{ba} I_a + Z_{bb} I_b \end{aligned} \right\} \quad (4)$$

The voltages V and the currents I of Eq. 1 are related to those of Eq. 4 (see Fig. VII-2) by

$$V = V_a, \quad I = -I_a \quad (5)$$

Introducing relation 5 and Eq. 1 into Eq. 4 and solving for V_b in terms of I_b we find

$$V_b = Z' I_b + E' \quad (6)$$

with

$$Z' = -Z_{ba}(Z + Z_{aa})^{-1} Z_{ab} + Z_{bb} \quad E' = Z_{ba}(Z + Z_{aa})^{-1} E \quad (7)$$

Equation 6 represents the properties of the transformed network. If the transformation is lossless, but not necessarily reciprocal, we must have

$$-Z_{aa} = Z_{aa}^+, \quad -Z_{bb} = Z_{bb}^+, \quad -Z_{ab} = Z_{ba}^+ \quad (8)$$

It is not hard to show that the general transformation of the impedance matrix and noise matrix Eq. 7 can be broken down into three steps (ref. 1 gives a discussion that can easily be generalized to the nonreciprocal case). The three basic steps, with the assumption of a lossless transforming network, are:

1. $Z' = Z + Z_{kk}$ $E' = E$ with $Z_{kk} = -Z_{kk}^+$
2. $Z' = Z^{-1}$ $E' = Z^{-1} E$
3. $Z' = TZT^+$ $E' = TE$ with T arbitrary

Step 1 (with $Z_{kk} = Z_{aa}$), step 2, step 3 (with T interpreted as Z_{ab}), and step 1 (with $Z_{kk} = Z_{bb}$), performed in the succession indicated leads to the general transformation Eq. 7. We shall now show that the matrix N defined by Eq. 3 undergoes a similarity transformation when any one of the three transformations listed above is applied to it.

Step 1 leaves N unaffected, since $Z' + Z'^+ = Z + Z^+$ and $E = E'$. Under step 2, we obtain

$$\begin{aligned} N' &= \overline{E'E'^+} (Z' + Z'^+)^{-1} = Z^{-1} \overline{EE^+} (Z^+)^{-1} \left[Z^{-1} + (Z^+)^{-1} \right]^{-1} \\ &= Z^{-1} \overline{EE^+} (Z + Z^+)^{-1} Z = Z^{-1} N Z \end{aligned} \quad (9)$$

Equation 9 shows that N' and N are related by a similarity transformation. Such a

transformation leaves the eigenvalues of N invariant. Under step 3, we obtain

$$N' = T \overline{EE^+} T^+ (TZT^+ + TZ^+ T^+)^{-1} = T N T^{-1} \quad (10)$$

Since the operation in Eq. 10 is also a similarity transformation, we have proved that the transformation (Eq. 7) leaves the eigenvalues of N invariant. The number of invariants of the N matrix is thus equal to, or less than, n .

Work is in progress on the interpretation of the noise invariants. So far it has been confined to two terminal-pair networks. It has been shown that the noise performance of conventional amplifiers is intimately connected with one of the eigenvalues of N . Consider, for example, the case when the matrix $Z + Z^+$ is neither positive nor negative definite. This is the case for all but the negative resistance amplifiers (1). Since $\overline{EE^+}$ is a positive definite matrix, the two eigenvalues of the N matrix are of opposite sign. When the amplifier is put into its unilateral form by a lossless feedback scheme (1), the minimum value of the expression

$$M = (F-1)/(1 - 1/G)$$

(where F is the noise figure, G is the available power gain) is given uniquely in terms of the negative eigenvalue N_- of the matrix N and

$$M_{\text{opt}} = |N_-|/2kT\Delta f \quad (11)$$

In the case of a lossless, microwave, longitudinal-beam tube, N_- is related to the uncorrelated noise component in the slow-beam wave (2). In the notation of reference 3

$$|N_-| = 4\pi\Delta f(S - \Pi)$$

An investigation is in progress as to whether the optimum value for M (see Eq. 11) is an ultimate limit of the noise performance of the amplifier imbedded in an arbitrary lossless network.

If the generators E are all perfectly correlated (signal process), the matrix $\overline{EE^+}$ is of rank unity. The matrix N is therefore of rank unity (or zero in a trivial case). Thus the matrix N has only a single invariant. This invariant has a particularly simple meaning, as will be shown now for a general n terminal-pair network.

If the network with the single-frequency signal generators E is fed with n current generators characterized by the column matrix I , the power absorbed by the network is

$$P = \frac{1}{4} (V^+ I + I^+ V) = \frac{1}{4} [I^+ (Z + Z^+) I + E^+ I + I^+ E] \quad (12)$$

Equation 12 describes the power as a quadratic surface in the space of the currents I . The linear terms in Eq. 12 can be eliminated by a proper translation of coordinates. Setting $I' = I + (Z + Z^+)^{-1} E$ and introducing this transformation into Eq. 12, we obtain

(VII. MICROWAVE ELECTRONICS)

$$P = I'^+(Z + Z^+) I' - E^+(Z + Z^+)^{-1} E \quad (13)$$

A minimum, maximum, or saddlepoint of the surface Eq. 13 is reached when $I' = 0$. The remaining constant is the height of the extremum. If the network is passive, $-E^+(Z + Z^+)^{-1} E$ is negative and represents the maximum available power obtainable from the internal generators of the network. If the network is capable of the generation of power as well as the absorption of it in the absence of the internal generators, the extremum is a saddlepoint of the surface. Furthermore, $E^+(Z + Z^+)^{-1} E$ is the trace of the matrix $N = \overline{EE^+(Z + Z^+)^{-1}}$. Since N is of rank unity or less in the case of a signal process, the trace of N is also equal to its single nonzero eigenvalue and thus it is equal to the only invariant of the M matrix.

H. A. Haus, R. B. Adler

References

1. S. J. Mason, Power gain in feedback amplifiers, Technical Report 257, Research Laboratory of Electronics, M.I.T., August 25, 1953.
2. Quarterly Progress Report, Research Laboratory of Electronics, M.I.T., July 15, 1955, p. 26.
3. H. A. Haus and F. N. H. Robinson, Minimum noise figure of microwave beam amplifiers, Proc. IRE 43, 981 (August 1955).

2. Shot Noise in Transistors

In the search for an interpretation of the noise parameters discussed in the preceding section a study has been started on shot noise in transistors. The recently published theory of North gives us the fundamental principles (1). It is hoped that the connection between the noise and gain mechanisms in a transistor will be clarified as a result of this work.

A simple expression is obtained for the noise invariant N_- of Section VII-B.1 by using the equivalent noise generators of the transistor circuit in reference 1. Neglecting the Early effect and disregarding the base resistance ($\mu_{ec} = \mu_{bc} = r'_b = 0$), we have for N_-

$$N_- = \left(\frac{1}{2} kT \Delta f \right) \left[\frac{1 + 4 \left(\frac{1-a}{a} \right) |u|^2 + \left(1 - 8 \left(\frac{1-a}{a} \right) |u|^2 + 16 \frac{1}{a} \left(\frac{1-a}{a} \right) |u|^4 \right)^{1/2}}{|u|^2 - 1} \right]$$

where $|u|^2 = a^2 r_c / 4r_e$. This result shows that in a transistor the gain and noise are intimately related. Even under the stringent assumptions given above, N_- is finite except for $r_c / r_e = \infty$. In this case, however, no current is required to achieve a finite power gain, and thus no shot noise is introduced.

B. W. Faughnan

References

1. A. Van der Ziel, Theory of shot noise in junction diodes and junction transistors, Proc. IRE 43, 1639 (Nov. 1955).

C. DENSE BEAM STUDIES

1. High-Perveance, Cylindrical Electron Beams

At the present time, most high-power longitudinal beam tubes operate with perveances less than 3×10^{-6} amp/volt^{3/2}. If tubes could be built to operate efficiently with higher perveances an appreciable reduction in the voltage requirements would become feasible. Several theoretical analyses of cylindrical beams will be found in references 1-7. As an extension to the work of various authors a number of curves have been calculated and plotted to alleviate some problems in future design. The notation used is as follows:

K = perveance in amp/volt ^{3/2}	V_4 = drift-tube potential
r_4 = drift-tube radius	V_3 = beam potential at r_3
r_3 = outside radius of the beam	V_2 = beam potential at r_2
r_2 = inside radius of the beam	V_m = minimum beam potential.

In confined-flow beams (2, 4, 5, 6) the maximum perveance occurs when $V_2/V_4 = V_m/V_4 \approx 1/3$. Figure VII-3 shows the variation of this limiting perveance as a function of the drift-tube radius to beam radius ratio r_4/r_3 . For hollow beams the ratio r_3/r_2 is the parameter. At values of limiting perveance, longitudinal slip becomes excessive in most applications. Therefore, the perveances were recalculated with V_m/V_4 as parameter. Figure VII-4 shows curves for a solid beam and Fig. VII-5 for a hollow one with $r_3/r_2 = 1.2214$. Curves have also been plotted for other values of the r_3/r_2 ratio.

The variations of V_m/V_3 when V_m/V_4 is the parameter have been calculated and plotted to take into consideration the fact that the percentage of slip is proportional to $(V_m/V_3)^{1/2}$ rather than to $(V_m/V_4)^{1/2}$. The unpublished calculations show that in a confined-flow beam the perveance must be considerably less than the limiting value whenever rigid slip specifications are imposed. The perveance can be considerably larger in a tubular beam, provided that the beam is thin and the ratio of the drift-tube radius to beam radius is close to unity.

In a Brillouin focused beam (1, 3, 7) all electrons have the same longitudinal-velocity component, and the excess energy of the outer electrons is taken up by rotation about the axis of the beam. In a solid Brillouin focused beam the charge distribution is uniform across the beam, which rotates as a unit. Figure VII-6 shows the limiting perveance of the solid Brillouin focused beam as a function of the ratio of drift-tube radius to beam radius.

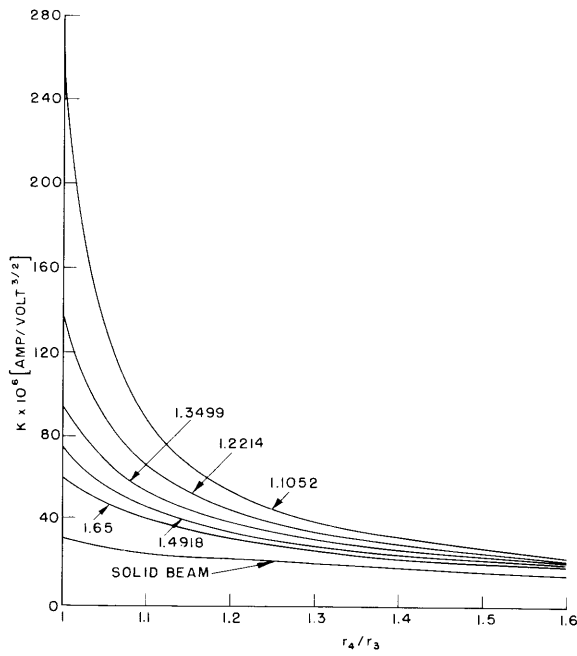


Fig. VII-3. Limiting perveances of confined-flow electron beams with parameter r_3/r_2 for tubular beams.

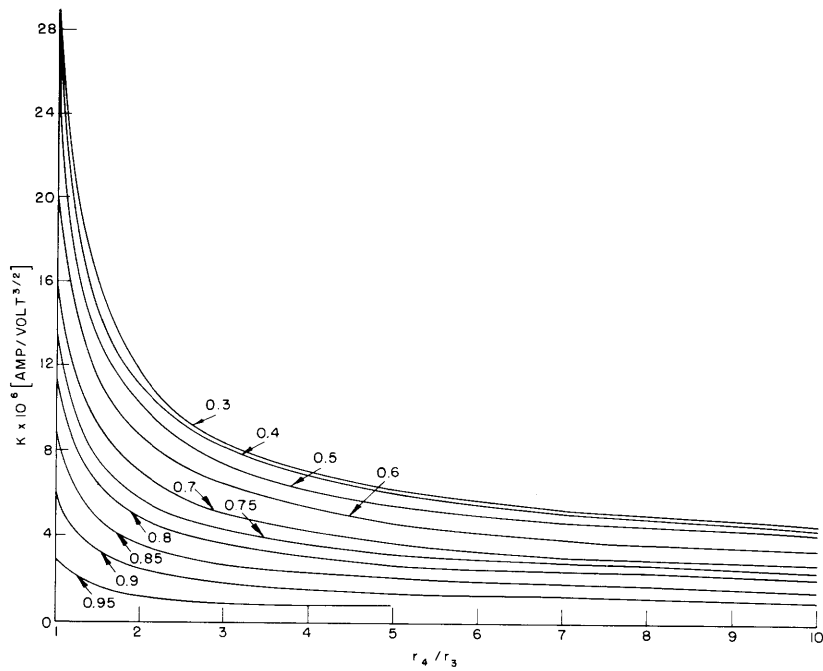


Fig. VII-4. Perveance of confined-flow solid beams with parameter V_m/V_0 .

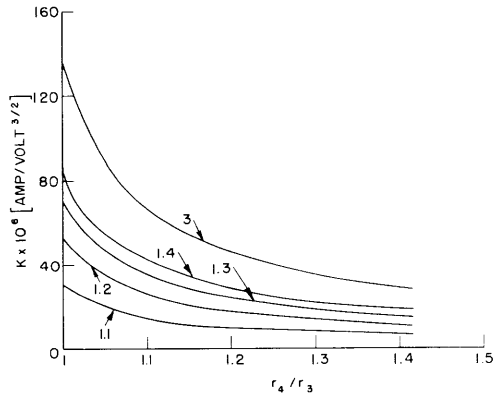


Fig. VII-5. Perveance of confined-flow tubular beam for $r_3/r_2 = 1.2214$, with parameter V_4/V_2 .

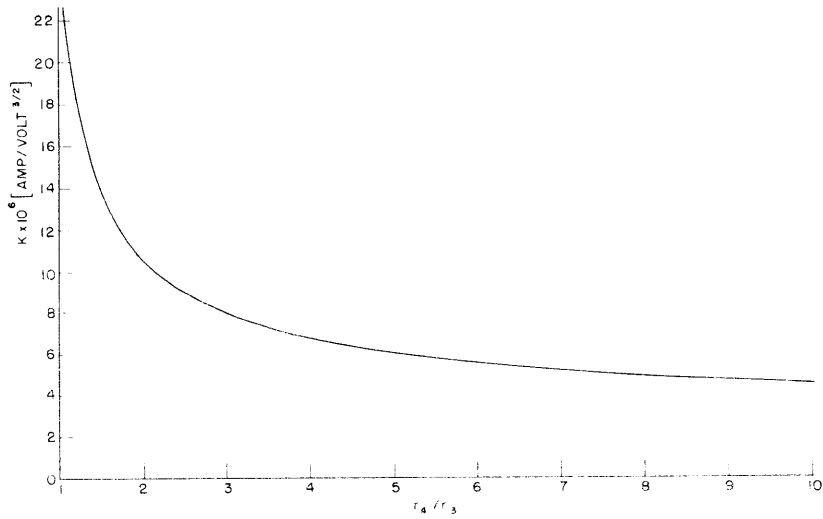


Fig. VII-6. Limiting perveance of Brillouin focused solid beam.

(VII. MICROWAVE ELECTRONICS)

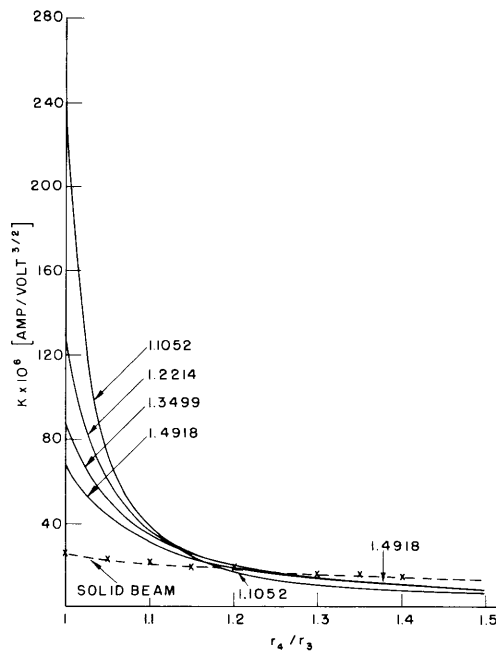


Fig. VII-7. Limiting perveance of Brillouin focused tubular beam with parameter r_3/r_2 .

In a hollow Brillouin focused beam a nonuniform charge distribution is required for stable solutions. All of the focusing flux lines lying within the inner-beam diameter in the uniform field region must thread through a hole in the cathode (7). The angular velocity becomes a function of the radius in a hollow beam; its value is maximum at the outer edge and zero at the inner edge. The maximum perveance occurs at $V_2/V_3 = V_m/V_3 \approx 1/3$, just as in confined-flow beams. Figure VII-7 shows the limiting perveance for Brillouin focused beams as a function of the ratio of the drift-tube radius to beam radius, with r_3/r_2 as the parameter for tubular beams.

A demountable vacuum system has been designed for future studies of high-perveance beams. The system is under construction.

C. Fried

References

1. A. L. Samuel, Proc. IRE 37, 1252-58 (1949).
2. N. Wax, J. Appl. Phys. 20, 111-123 (1947).
3. C. C. Wang, Proc. IRE 38, 135-47 (1950).
4. L. T. Smith and P. L. Hartman, J. Appl. Phys. 11, 220-29 (1940).
5. D. P. R. Petrie, Elec. Communication 20, No. 2, 100-111 (1941).
6. J. R. Pierce, Theory and Design of Electron Beams (D. Van Nostrand Company, Inc., New York, 2nd ed., 1954).
7. L. A. Harris, Technical Report 170, Research Laboratory of Electronics, M.I.T., Aug. 1950.

D. KLYSTRONS

1. Distributed Klystron Theory

Theoretical work has been started on the amplifying characteristics of longitudinal-beam tubes in which an interaction structure is located periodically along the beam. The first interaction structure to be treated was a klystron resonant cavity with associated drift regions. Some of the results of this investigation are summarized below.

a. Electrons in quasi-static fields

The gaps of klystron cavities through which the electrons pass are usually "short" in the sense that $z_{\text{gap}} \ll \lambda/4$ (λ is the operating wavelength), and $z_{\text{gap}} \ll \lambda_q/4$ (λ_q is the plasma wavelength). The electric field in such a gap can be considered quasi-static, and space-charge fields can be neglected in a first approximation. The effect of a cavity upon a modulated electron beam that passes through its gap can be represented by a two terminal-pair transformation (Fig. VII-8) as follows:

$$\begin{pmatrix} V_2 \\ I_2 \end{pmatrix} = \begin{pmatrix} (y_5 + ay_4) & \frac{ay_4^2}{Y_2} \\ (Y_3 + aY_2) & (y_5 + ay_4) \end{pmatrix} \begin{pmatrix} V_1 \\ I_1 \end{pmatrix} \quad (1)$$

where V_1 and V_2 are the kinetic voltages, and I_1 and I_2 are the currents in the beam at the input and output of the gap, respectively. The gap parameters in this matrix are:

$$Y_{e1} = \frac{1}{2} G_o y_1 \quad y_1 = \frac{2}{\theta^2} (1 - e^{-j\theta}) - \frac{j}{\theta} (1 + e^{-j\theta})$$

$$Y_2 = \frac{1}{2} G_o y_2 \quad y_2 = \frac{j}{\theta} (1 - e^{-j\theta}) + e^{-j\theta}$$

$$Y_3 = \frac{1}{2} G_o y_3 \quad y_3 = j\theta e^{-j\theta}$$

$$y_4 = -M e^{-j\theta/2} \quad M = \frac{\sin(\theta/2) I_o(\gamma b)}{\theta/2 I_o(\gamma a)}$$

$$y_5 = e^{-j\theta/2} \quad G_o = \frac{I_o}{V_o}; \theta \text{ is the transit angle}$$

$$a = -\frac{Y_2}{Y} \quad Y = Y_g + Y_{e1}; Y_g \text{ is the cavity admittance at the gap}$$

(VII. MICROWAVE ELECTRONICS)

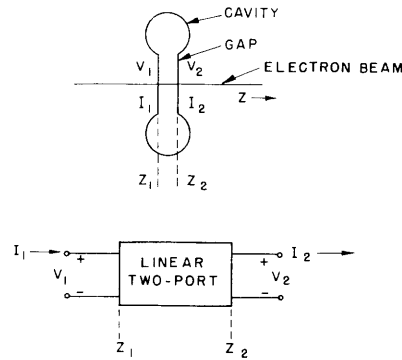


Fig. VII-8. Small-signal interaction of electrons with cavity gap-fields.

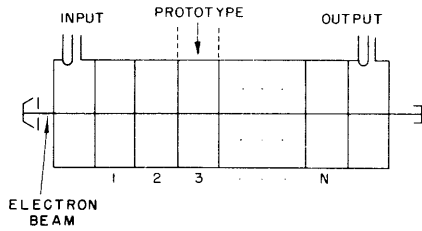


Fig. VII-9. Distributed klystron consisting of a series of N+2 uncoupled resonators.

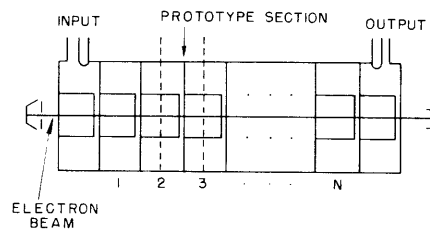


Fig. VII-10. Distributed klystron consisting of a series of reentrant-type resonators.

For an electron beam passing through a "short" drift region, with no applied rf field, we have

$$\begin{pmatrix} V_2 \\ I_2 \end{pmatrix} = \begin{pmatrix} y_5 & 0 \\ Y_3 & y_5 \end{pmatrix} \begin{pmatrix} V_1 \\ I_1 \end{pmatrix} \quad (2)$$

where the parameters are functions of the "short" drift length.

b. Gain of amplifiers

Equations 1 and 2 describe the basic "short" klystron structure. We choose a cavity gap and associated drifts to form a prototype of our structure. These structures, let us say (N+2) of them, are placed successively along the electron beam. The first structure excites the system. The N following structures can be considered to propagate an exponentially growing wave, in the usual sense of wave analysis in periodic structures. The last structure extracts power from the beam and delivers it to a load.

The gain of such an amplifier can be written (if $N\Gamma \gg 1$)

$$\text{GAIN} = N\Gamma + K + L \quad \text{db} \quad (3)$$

where N = number of intermediate structures, Γ = power gain of the growing wave per structure (db), K = power gain in the first and last structure (db), and L = initial power loss in the excitation of the growing wave (-db). The intermediate structures can be described by general circuit parameters (ABCD) which follow from suitable products of the matrices of Eqs. 1 and 2. For symmetrical structures ($A = D$), the power gain of the growing wave per structure is

$$e^{2\gamma} = A^2 \left[1 + \left(1 - \frac{\Delta}{A^2} \right)^{1/2} \right]^2 \\ \approx 4A^2 \quad (4)$$

where Δ is the determinant of the structure matrix. A straightforward derivation of the quantities corresponding to K and L can be taken from their definitions given above. Two examples of practical importance are given below.

Prototype (a): Finite gap cavity, no drift regions.

The amplifier consists of a series of $N + 2$ uncoupled resonators as shown in Fig. VII-9. For a matched input and output and operation at the resonant frequency of the cavities, the gain is

$$\text{GAIN} = |\alpha|^2 \frac{|y_4|^4 |Y_2|^2}{4G^2} |e^{N\gamma}|^2 \quad (5)$$

where

$$e^\gamma \approx 2A; \quad A = \frac{1}{\Delta} (y_5 + ay_4) \quad \text{and} \quad \Gamma = 10 \log_{10} |e^\gamma|^2$$

$$\alpha = \frac{1}{2} \left[1 - \left(1 - G \frac{Y_3}{Y_2} \right)^{1/2} \right] \quad \text{and} \quad L = 10 \log_{10} |\alpha|^2$$

$$G = G_s + G_{el} \quad K = 10 \log_{10} \frac{|y_4|^2 |Y_2|^2}{4G^2}$$

Prototype (b): Infinitesimal gap cavity, "short" drift regions before and after the gap.

The amplifier then has $N + 2$ re-entrant-type cavities as shown in Fig. VII-10.

(VII. MICROWAVE ELECTRONICS)

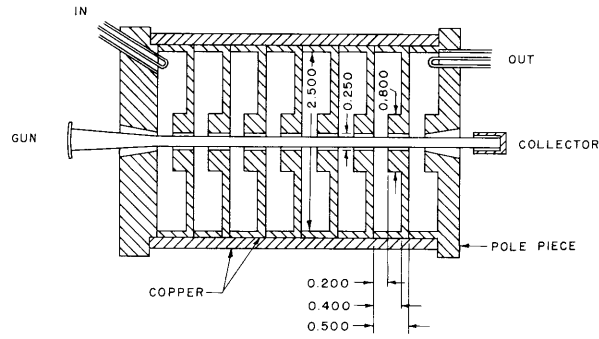


Fig. VII-11. Distributed klystron.

Under the same operating conditions listed above, in prototype (a) the gain is

$$\text{GAIN} = |\alpha|^2 \frac{|Y_3|^2}{4G^2} |e^{N\gamma}|^2 \quad (6)$$

where

$$e^{\gamma} \approx 2A; \quad A = 1 - j \frac{1}{2} \theta \frac{G_0}{G}$$

$$\alpha = 1 - \frac{1}{2} \left(\rho + \frac{1}{\rho} \right); \quad \rho = 1 + j \frac{4}{\theta} \frac{G}{G_0}$$

$G_0 = \frac{I_0}{V_0}$ and $\theta =$ the transit angle of the drift. Γ , L , and K can be identified as

before.

Considerations of space-charge, bandwidth, and response will be reported later.

A. Bers

2. Distributed Klystrons

For the purpose of testing some of the analytical work described in Section VII-D.1, a short distributed klystron illustrated by Fig. VII-11 is being built. It will use a 10-kv pulsed gun (perveance 10^{-6}) obtained from the General Electric Laboratories at Stanford, California. The tube is under construction.

B. A. Highstrete, L. D. Smullin

E. PHASE BUNCHING FOR A SYNCHROTRON

Radial oscillations are set up in a synchrotron by phase variance and energy variance around the phase-stable particle at the input. In order to reduce the amplitude of these oscillations we shall try to bunch the particles in phase with as little energy spread as possible. The dynamics of phase bunching is being studied in the context of the optimization of the performance of a complete injector system.

A. J. Lichtenberg